

Inner Annular Gap and Related Topics

K. J. Lee¹*, G. J. Qiao¹, H. G. Wang², B. Zhang³ and R. X. Xu¹

¹ Department of Astronomy, Peking University, Beijing 100871, China

² Center for Astrophysics, Guangzhou University, Guangzhou 510400, China

³ Department of Physics, University of Nevada, Las Vegas, Nevada 89154, USA

Abstract Geometrical properties of the annular gap model, efforts of observational tests on it and applications of the model to explain the bi-drifting phenomenon are introduced in this paper. It was shown that in the frame of the annular gap model the observed γ -ray and radio radiation properties of pulsars can be well reproduced. The annular gap model can naturally explain the bi-drifting phenomenon, which is difficult to be understood in classical inner vacuum models. Recently, Wang et al. proposed an independent geometrical method to determine the location for the multi-band radiation regions of PSR B1055–52. They found that the γ -ray emission and radio main pulse emission come from the annular gap, while the radio inter-pulse originates from the core cap region. The results show that the constrained radio and γ -ray emission regions are generally consistent with the predictions of the annular gap model.

Key words: pulsars: general — pulsars: individual (PSR J0815+09, PSR B1055–52) — radiation mechanisms: non-thermal — stars: neutron — elementary particles

1 INTRODUCTION

The physics for the origin of γ -ray from the rotational-powered pulsar is still unclear today, although numerous efforts have been made on this topic. The early works on this topic date back to 1970s (Sturrock 1971; Ruderman & Sutherland 1975), when people have already realised that different cases of binding energy of the charged particles on stellar surface result in different kinds of acceleration gaps. In literature three main kinds of gap models were proposed, i.e. the free-flow models (Sturrock 1971; Arons 1983; Harding & Muslimov 1998), which assume negligible binding energy on stellar surface, the sparking gap models (Ruderman & Sutherland 1975), which assume high binding energy on the stellar surface, and the outer gap models (Holloway 1973; Cheng et al. 1986; Chiang & Romanni 1994), which assume that the charge deficient gap locates near the null charge surface (NCS). These models are successful in accounting for some observational facts, but these models also meet problems. Some of them are related to geometrical properties. Both the free-flow and the sparking gap models suggest that the γ -ray radiation regions locate near the stellar surface and there is no further acceleration for charged particles. Thus, they predict narrow γ -ray radiation beams. Small inclination angles are required for pulsars to generate observed wide γ -ray light curves, which may not be always true. For outer gap models, the γ -ray beam is suggested to be fan-like wide beam, thus the wide light curves can be explained without requirement special inclination angles. But it's difficult for the outer gap model to explain the observed off-pulse γ -ray radiation as observed in some pulsars, e.g. the Crab pulsar. To avoid the geometric problems, Qiao et al. (2003, 2004a) proposed the annular gap model (IAG), which suggests that the radiation regions are extended from stellar surface to the heights close to (may beyond) the NCS. They further point out that IAG models also works well for radio pulsars. At same time, Dyks et al. (2003) proposed a so-called caustic model, which assume that the

* E-mail: k.j.lee@water.pku.edu.cn

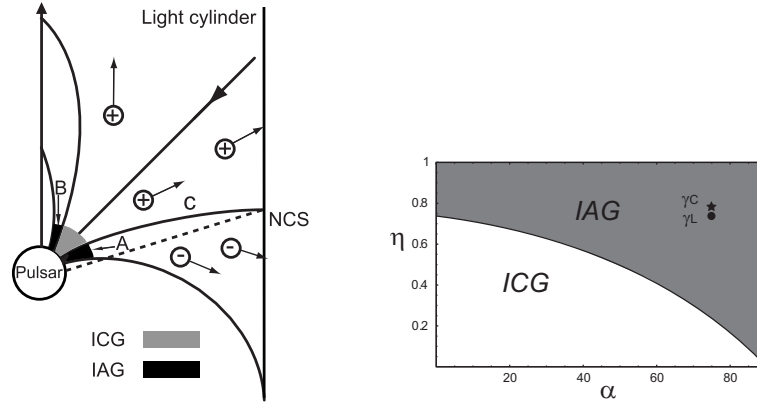


Fig. 1 Left panel: The position of the inner annular gap (IAG) region and the inner core cap (ICG) region. The null change surface (NCS) is the surface where the magnetic field perpendicular the axis (i.e. $\Omega \cdot \mathbf{B} = 0$). It can be seen that only if the radiation location near the NCS, wide radiation beam is plausible. Right panel: The curve is the ratio η between the maximal radius of core gap and annular gap respected to inclination angle α , which is in unit of degree. This curve separates the whole parameter space into two parts, the upper part (shadowed) belongs to the inner annular gap, while the lower part belongs to the inner core gap, as marked in the figure. The dot and star symbol are the parameters for the γ -ray radiation region of the PSR B1055–52 derived by Wang et al. (2005). The star symbol indicates the η parameter of the central γ -ray radiation position; and the dot symbol indicates the η of the leading γ -ray radiation position.

radiation region is extended from star surface to places near the light cylinder. They show that such a pure geometric model can successfully reproduce the observed γ -ray properties of pulsars.

To test the validity of the physical picture of the IAG model, Wang et al. (2005) proposed an independent geometric method to constrain the 3-D structure of emission regions by fitting both the radio and high energy observations. Applying this method to the γ -ray pulsar PSR B1055–52, it is revealed that the radio emission region probably consists of an inner and an outer ring, while the γ -ray emission region is beyond the NCS and severely asymmetrical to magnetic axis. The results show that the radiation location for PSR B1055–52 is consistent with the prediction of annular gap model.

The geometrical aspects of annular gap model are introduced in Section 1. The geometric method to constrain radio and γ -ray emission regions and its application to PSR B1055–52 are outlined in Section 2. The application of the annular gap model to accounted for the subpulse bi-drifting phenomenon are described in Section 3. Discussions and conclusions are made in Section 4.

2 GEOMETRIC ASPECT OF ANNULAR REGION

The open field line region of the magnetosphere is divided by the critical field lines into two parts (Holloway 1975). One part containing the magnetic axis is called the core region and the other part is the annular region. The configuration of gaps is shown in the left panel of Figure 1.

Because the NCS is defined as a surface within light cylinder where $\Omega \cdot \mathbf{B} = 0$ is satisfied, only when the radiation location is near the NCS, could the pulsar beam become very wide. In this case, it is easy to see that a wide γ -ray emission beam should be produced by particles generated in the inner annular gap, because only such particles have the possibility of passing the NCS. Following Qiao et al. (2004a), the radiation height $r(\phi)$ defined as the distance from a emission point to stellar center is expressed as $r(\phi) = \lambda \kappa r_N(\phi) + (1 - \lambda) \kappa r_N(0)$, where ϕ is the azimuthal angle, $r_N(\phi)$ is the height between stellar center and the intersection of a last open magnetic field line and the NCS, $r_N(0)$ denotes the height of the NCS on the plane whose $\phi = 0$, κ and λ are free parameters. Once κ and λ are given, the radiation geometry of pulsar is fixed. The physical meaning of κ is the non-dimensional height of radiation positions in unit of $r_N(\phi)$. λ is a correction factor.

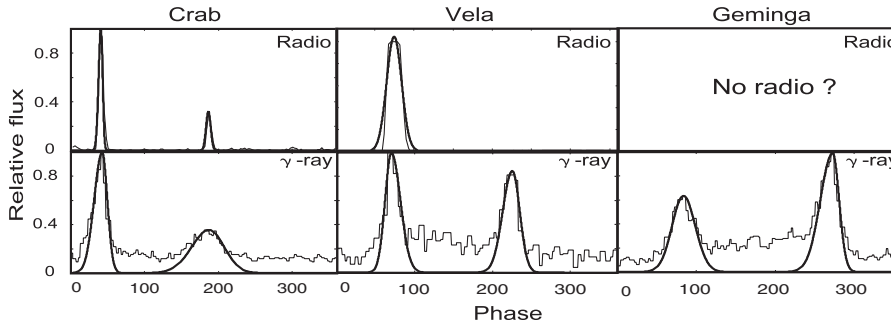


Fig. 2 The simulated and observed Crab-like, Vela-like and Geminga-like light curve at both radio and γ -ray bands. The γ -ray and radio data are derived from Thompson 2003 and the European Pulsar Network Data Archive respectively. The parameters listed in the figure are just for reference. If phase separation is determined with 10% error, we found that $\alpha \in [36, 49]$, $\zeta \in [39, 57]$, $\kappa \in [0.8, 0.99]$, $\lambda \in [0.65, 0.85]$ for Crab and $\alpha \in [33, 44]$, $\zeta \in [51, 61]$, $\kappa \in [0.65, 0.83]$, $\lambda \in [0.77, 0.99]$ for Vela. We do not give parameters for Geminga light curve, the parameters can not get only from γ -ray light curve. Note: 1.) that the relative phase shift between radio and γ -ray bands are not plotted. 2.) Some groups detect the radio radiation from Geminga (Malofeev & Malov 1997).

Because charged particles with opposite signs leave off the light cylinder, as shown in Figure 1, a natural picture is that particles with opposite charges should leave off the annular and core cap region respectively, although the GJ charge density is the same in the inner annular and inner core gap regions. Figure 2 is derived from Qiao et al. (2004a). It shows that the simulation can match the geometrical features of observation well.

Another geometrical feature that support the annular gap region to be a efficient γ -ray emission region is the ratio η between the typical sizes of core cap and annular gap. The ratio η between the maximal radius of annular gap and core cap is approximately written as $\eta = r_{p,ICG}/r_{p,IAG} \simeq 0.74 - 0.0023\alpha$, where the definition of $r_{p,ICG}$ and $r_{p,IAG}$ can be found in Figure 4. Accurate results of η are given in right panel Figure 1. It shows that when the inclination angle is large, the size of annular gap become large compared with that of core cap region, so the potential drop in annular gap dominates that in core gap. In other words, the annular gap model prefer pulsar with large inclination angle. The right panel of Figure 1 also show that if observation can determine the parameter η and α for a given radiation component, it will provide a strong test for the gap models, i.e. it can answer the question if the radiation comes from the annular region or the core region.

3 OBSERVATIONAL CONSTRAIN ON ANNULAR GAP MODEL

Recently Wang et al. (2005) use an independent geometrical method to constrain the 3-D structure of radiation region of PSR B1055–52, which is a γ -ray pulsar with radio main pulse and inter-pulse. They focus on constraining the emission regions of PSR B1055–52 seen through the line of sight via fitting the observed emission properties. The main idea of the method is to relate the observational properties to the geometry of emission regions. In pulsar magnetosphere photons are emitted from a group of open field lines, thus forming multi-wavelength emission beams. (1) The observed pulse widths are related to beam size (or spatial extent of the emission regions) as well as the inclination angle α and the viewing angle ζ between the line of sight (hereafter LOS) and the rotation axis. (2) The observed phase offsets between various pulses are attributed to the original phase offsets due to the separation of field lines and the additional offsets caused by aberration and retardation effects. Both effects have relationships to the geometry of emission regions. (3) The position angle sweep of radio polarization is used to constrain α and ζ . Therefore, the geometrical parameters, i.e. the emission heights, the azimuthal angles of field lines ϕ and the fractional position ξ of open field lines within polar cap region (defined as the ratio of polar angle of the footprint of a open field lines on stellar surface to that of the footprint of the last open field line which has the same azimuthal angle) can be constrained for radio and γ -ray emission respectively by fitting those observational features.

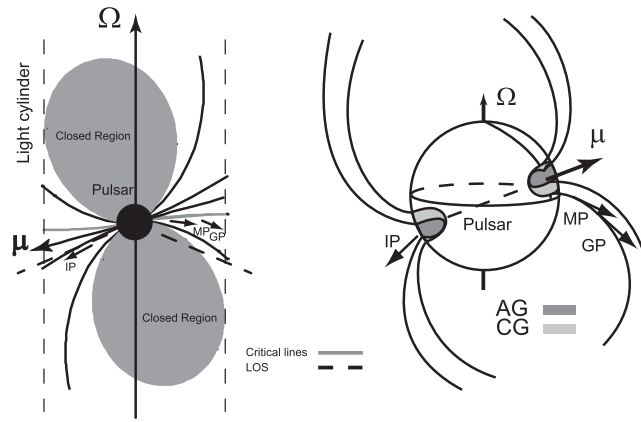


Fig. 3 The illustration for the origin of radio and γ -ray emission from the magnetosphere of B1055–52 according to the results derived by Wang et al. (2005). It shows that the γ -ray radiation comes from the annular region.

The results derived by Wang et al. is summarized as follows. (1) $\alpha = 75^\circ$ previously derived by Lyne & Manchester (1988) is confirmed. (2) For the γ -ray emission regions viewed by our line of sight, the emission heights are within $0.59r_c$ to $0.83r_c$, where r_c is the radius of light cylinder, the values of ξ are within $[0.7, 0.8]$. (3) Radio emission comes from two rings of open field lines in polar cap. The outer ring is composed of open field lines near the last open field line and corresponds to the observed main pulse, while the inner one consists of field lines very close to the magnetic axis with $\xi = 0.2 - 0.6$ and corresponds to the observed inter-pulse. Compare these results with right panel of Figure 1, it shows clearly that the γ -ray radiation for PSR B1055–52 does come from the annular region. Radio main pulse and inter-pulse probably originate from annular and core cap regions, respectively. An illustration for the geometrical model of PSR B1055–52 is shown in Figure 3.

The method mentioned above relies on assumptions that the magnetic field is pure dipole and the radio and γ -ray emission regions are approximately symmetrical to the plane that contains the rotation and magnetic axes. In next step it should be developed to apply to more realistic magnetic field configuration that involves magnetic sweep back effect and abandon the symmetry assumption about the emission regions. An improved method has been used for PSR B1055–52. The preliminary results are reported by Wang et al. in this symposium, which generally support the IAG model and meanwhile reveal some interesting asymmetrical properties of the emission regions.

4 BI-DRIFTING

A unique bi-drifting phenomenon was discovered in radio emission from PSR B0815+09 (McLaughlin et al. 2004), which shows two opposite drifting directions within four components of the average pulse profile. In the frame of the IAG model, it is found that the bi-drifting could be explained successfully (Qiao et al. 2004b)

For the inner gaps, the typical gap height is smaller than the polar cap radius, and one can use the 1-D approximation of the Poisson equation in the co-rotate frame, i.e. $\partial E_{\parallel} / \partial x = 4\pi(\rho - \rho_{GJ})$, where x is the longitudinal distance measured from the surface along the curved magnetic field lines, and E_{\parallel} is the parallel component of the electric field with respect to the magnetic field, ρ is the charge density and ρ_{GJ} is the GJ charge density. This equation governs the electric field along the magnetic field (i.e. segments “ab”, “ch”, “dg” and “ef” in Figure 4). The boundary condition equation is $E_{\parallel} = 0$ at the upper boundary of the gap (i.e. segment “edcb”).

When the gaps are re-generated after each sparking process, since opposite charged particles leave the ICG and the IAG regions, respectively, the sign of $\rho - \rho_{GJ}$ is the opposite in the two gaps. The Poisson

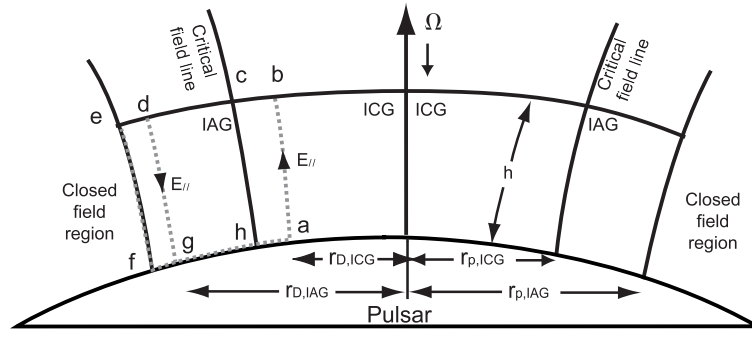


Fig. 4 The annular gap (IAG) and the inner core gap (ICG). $r_{p,IAG}$ and $r_{p,ICG}$ are the radii of the IAG and the ICG, respectively. The two gaps are divided by the boundary line ‘ch’, which is the critical magnetic line that passes through the intersection of the null-charge line and the light cylinder. The dashed lines are used to illustrate the electric property of the gaps discussed in section 2. The parameters used in our simulations are presented in the text.

equation above shows that the directions of $E_{||}$ are also different in the IAG and ICG. We expect that at the boundary between ICG and IAG (line “ch”) the parallel electric field vanishes. That is $\int_c^h E \cdot ds = 0$.

We handle the electrodynamics in the co-rotate frame. For any close circuits (e.g. “defg”, “abch”), one has $\oint E \cdot ds = 0$. In the closed magnetic field region $E \cdot B = 0$, so $\int_e^f E \cdot ds = 0$. As discussed in RS75, we have $\int_f^g E \cdot ds = 0$. Thus for the IAG, one has $\int_g^d E \cdot ds + \int_d^e E \cdot ds = 0$. When considering the boundary condition between the two gaps one has $\int_c^h E \cdot ds = 0$. Also $\int_h^a E \cdot ds = 0$ is satisfied for the same reason as in the discussion of the IAG case. One can get $\int_a^b E \cdot ds + \int_b^c E \cdot ds = 0$. Therefore for the IAG and the ICG the perpendicular electric field is directly linked to the parallel electric field. Because the parallel electric fields in the IAG and the ICG have different directions (i.e. $\int_a^b E \cdot ds$ and $\int_g^d E \cdot ds$ have different signs), the perpendicular electric fields in the two gaps are also different. The drifting velocity $v = E \times B / |B|^2$ have opposite signs in the ICG and the IAG, because the direction of magnetic fields is the same in the two gaps. This proposes a fundamental physical process to understand the bi-drifting phenomenon. The average drifting period is given by $\hat{P}_3 \simeq r_D B / 4ch(\rho - \rho_{GJ})$ where the r_D is the radius of the drifting path.

Besides the drifting direction, taking appropriate values of some parameters, the observed drifting rate along two directions can also be reproduced approximately. Detailed parameters and treatment are referred to Qiao et al. (2004b). It should be noted that there are still some uncertainties that may influence the theoretical modelling. We just estimate the averaged electric properties of gap region above. But the detailed drifting path and velocity definitely depend on detail factors. For example, the magnetic fields near the stellar surface may not be pure dipole (Gil & Melikidze 2002), additionally the real case of electric field is 3-D rather than 1-D. Thus the local drifting period may deviates from the estimation given above. In this way, polarisation observation for this pulsar can be helpful to test the annular gap model.

5 CONCLUSIONS AND DISCUSSION

1. The annular region is important for the γ -ray emission from pulsar. If radiation comes from the annular region, the radiation beam could be very wide. Given proper geometrical parameters, the IAG model can match observed γ -ray pulse profile for known pulsars very well.
2. From an independent geometrical method, the geometrical parameter of γ -ray pulsar B1055–52 are well constrained. It is demonstrated that PSR B1055–52 is a star which generate γ -rays from annular region. The details of the annular gap model for B1055–52 are still under-construction. An important question is whether annular gap model can pass the future detailed geometrical test from multi-band observation for other γ -ray pulsars, which proposed by Wang et al. 2005.

3. Bi-drifting phenomenon, which could not be well understood within traditional single cap model, can be naturally understood within the frame of annular gap model. But the detailed drifting velocity may deviate from present estimation due to some uncertainties. How to test annular gap model via fitting bi-drifting is still an incompletely settled question. The polarisation observation may provide a helpful way for such purposes.

Acknowledgements We are very grateful to Dr. Han, J. L. and Mr. Zhu W.W. for their valuable discussions. This work is supported by NSFC of China (10373002, 10403001 and 10273001).

References

- Cheng, K. S., Ho, C., Ruderman, M., 1986, ApJ, 300, 500
Chiang, J., Romani, R. W., 1994, ApJ, 436, 754
Dyks, J., Rudak, B., 2003, ApJ, 598, 1201
Gil, J., Melikidze, G. I., 2002, ApJ, 577, 909
Gil, J., Sendyk, M., 2000, ApJ, 541, 351
Harding, A. K., Muslimov, A. G., 1998, ApJ, 508, 328
Holloway, N. J., 1973, Nature, 246, 6
Holloway, N. J., 1975, MNRAS, 171, 619
Malofeev, V. M., Malov, O. I., 1997, Nature, 389, 697
McLaughlin, M. A., Lorimer, D. R., Champion, D. J., et al., 2004, in Young Neutron Stars and Their Environments IAU Symposium, Vol. 218 (eds. F. Camilo and B. M. Gaensler) (astro-ph/0310454)
Qiao, G. J., Lee, K. J., Wang, H. G., Xu, R. X., 2003, High Energy Processes and Phenomena in Astrophysics, Proceedings of the 214th Symposium of the International Astronomical Union held at Suzhou, China, 6-10 August, 2002. Edited by X.D. Li, V. Trimble, and Z.R. Wang. Published on behalf of the IAU by the Astronomical Society of the Pacific, 2003, p.167
Qiao, G. J., Lee, K. J., Wang, H. G., Xu, R. X., Han, J. L., 2004a, ApJ, 606, L49
Qiao, G. J., Lee, K. J., Zhang, B., Xu, R. X., Wang, H. G., 2004b, ApJ, 616, L127
Ruderman, M. A., Sutherland, P. G., 1975, ApJ, 196, 51
Sturrock, P. A., 1971, ApJ, 164, 529
Wang, H. G., Qiao, G. J., Xu, R. X., Liu, Y., 2005, MNRAS, 366, 945